Environmentally benign etching process of amorphous silicon and tungsten using species evaporated from polytetrafluoroethylene and fluorinated ethylene propylene

Kazushi Fujita, Masaru Hori,[a] and Toshio Goto
Department of Quantum Engineering, Graduate School of Engineering, Nagoya University, Furo-cho, Chikusa-ku, Nagoya 464-8603, Japan

Masafumi Ito
Department of Opto-Mechatronics, Faculty of Systems Engineering, Wakayama University, 930 Sakaedani Wakayama 640-8510, Japan

(Received 13 December 2001; accepted 28 October 2002; published 23 December 2002)

Environmentally benign etching process of amorphous silicon (*a*-Si) and tungsten (W) by using a plasma process with an evaporation of solid materials system has been developed for replacing a conventional plasma process using green house gases, such as SF_6 gas and perfluorocompound gases causing global warming. The evaporation system was designed to generate fluorocarbon species from solid materials by a CO_2 laser irradiation. An electron cyclotron resonance (ECR) plasma using O_2 accompanied with injection of species evaporated from solid materials has been applied to *a*-Si and W etching for cleaning process in chemical vapor deposition chamber. Fluorinated ethylene propylene (FEP) and polytetrafluoroethylene (PTFE) are selected as the solid material and the etching characteristics between FEP and PTFE have been compared. Furthermore, the etching of *a*-Si and W films has been performed in the divergent magnetic field ECR downstream plasma [electron density (n_e); $\sim 10^{10}$ cm^{-3}, electron temperature (T_e); 1.5–2.8 eV] and a planar ECR plasma [n_e; $\sim 10^{10}$ cm^{-3}, T_e; 3.4–4.4 eV] using O_2 gas with FEP evaporation. As a result, high etching rates of *a*-Si and W films of above 100 nm/min were successfully obtained at a substrate temperature of 400 °C in the planar ECR plasma of higher electron temperature. CF_x ($x=1$–3) radical densities and F atom density in plasmas were measured by an infrared diode laser absorption spectroscopy and an actinometric optical emission spectroscopy, respectively. On the basis of these measurements of species, the etching mechanisms of *a*-Si and W films are discussed. [DOI: 10.1116/1.1531131]

I. INTRODUCTION

Amorphous silicon (*a*-Si) and polycrystalline silicon (poly-Si) films have been generally synthesized by plasma-enhanced chemical vapor deposition. In addition, a tungsten (W) plug has been fabricated by etch back of W films deposited employing chemical vapor deposition (CVD) in ultralarge-scale integrated circuits processes. In these CVD processes, serious problems arise when *a*-Si, poly-Si, and W films are deposited on the chamber walls. These deposits on the chamber wall cause the excessive particle generation in the chamber. Therefore, these particles greatly influence the quality of films formed by CVD and the reproducibility of the CVD process. Plasma etching with SF_6 and perfluorocompound (PFC)/O_2 gases has been generally used for conventional chamber cleaning. In these chamber cleaning processes, F atoms generated from the electron impact dissociation of SF_6 and PFC gases play an important role in etching reactions of *a*-Si, poly-Si, and W films. SF_6 and PFC gases, however, cause a seriously environmental problem, namely global warming. The global warming potentials of these gases are estimated to be 6500–23 900 times as high as that of CO_2 gas and these gases have long lifetimes in the atmosphere. Therefore, the restriction of production of SF_6 and PFC gases is of vital importance and the use and production of SF_6 and some PFC gases in industries must be prohibited.

Recently, semiconductor industries have been taking some measures to reduce the negative impact of PFC gases on global warming. For example, the development of abatement systems for eliminating PFC gases emitted to the atmosphere has been investigated and feed gases with short lifetimes have been developed as alternative gases. However, conventional PFC gases and new alternative gases are usually supplied using gas cylinders. These gas cylinders have potential problems, such as a high risk of gas leakage during transportation and consumption. The legal restriction on gases requires a large waste gas disposal apparatus corresponding to the feed gas volume kept in gas cylinders. Moreover, the use of alternative gases is considered not to be the final solution for preventing global warming because the influence of species dissociated from alternative gases on the environment has not been known yet and these gases of short life times are basically dangerous for handling, which needs attachment of the extra system such as gas detector for safety.

In our previous study, we have proposed the novel etching system for environmental benignity without any PFC gases. Thus, the supply system of etching species, where fluorocar-

[a]Electronic mail: hori@nuee.nagoya-u.ac.jp

TABLE I. Structure, molecular weight, and melting temperature of each target.

Material	Structure	Molecular weight (g/mol)	Melting temperature (°C)
PTFE	$(-CF_2-CF_2-)_n$	10^7	327
FEP	$(-CF_2-CF_2-)_n(-CF_3CF-CF_2-)_m$	10^5	260

bon species were generated from polytetrafluoroethylene (PTFE) by a CO_2 laser evaporation, has been developed[1,2] and fluorocarbon species generated from the PTFE were injected into electron cyclotron resonance (ECR) O_2 plasma to produce F atoms through the dominant reaction of C_xF_y radicals and O atoms in the plasma. Therefore, this system employing solid material source is quite safe because of no risk for the leakage of fluorocarbon gases, very compact and furthermore never needs any gas cylinders, gas detectors and so on. This system has been successfully applied to the *a*-Si and W etching for chamber cleaning.[3]

Furthermore, by selecting various kinds of solid materials as an evaporation source, this method will enable us to investigate the new gas chemistry we have never observed in the plasma using the conventional fluorocarbon gases.

In this article, first, the etching of *a*-Si and W films was performed in a conventional divergent magnetic field ECR downstream plasma with two different type of solid material for PTFE and fluorinated ethylene propylene (FEP) as an evaporation source to compare their etching characteristics. The structure, molecular weight, and melting temperature of PTFE and FEP targets used in this study are shown in Table I. F/C ratio of FEP is 2.0, which is equal to that of PTFE. However, only difference of structure is that FEP has the side chain of CF_3 added partially to the main chain of PTFE. Second, in order to investigate the etching chemistry, CF_x ($x=1-3$) radical densities and F atom density in the plasma were measured by an infrared diode laser absorption spectroscopy (IRLAS) and an actinometric optical emission spectroscopy (AOES), respectively. On the basis of these measured results of species, the etching mechanisms of *a*-Si and W films are discussed. Third, etching characteristics using the conventional divergent magnetic field ECR plasma source were also compared with that using the planar ECR plasma source with permanent magnets with higher electron temperature under the condition of identical electron densities in the FEP evaporation. In addition, the dependence of etching rates on substrate temperature has been investigated using the planar ECR plasma with the FEP evaporation.

II. EXPERIMENT

The process chamber made of stainless steel was 40 cm in diameter and 40 cm in height. In this study, two types of plasma sources of conventional divergent magnetic field ECR plasma source and planar ECR plasma source (Iriekoken ECR-150D) employing permanent magnets were used. Figure 1 shows (a) a conventional divergent magnetic field ECR plasma system, (b) a planar ECR plasma process system, and (c) a top view of process chamber. In the conventional divergent magnetic field ECR plasma system, two magnet coils were arranged and they provided a divergent magnetic field. A 2.45 GHz microwave was introduced into the top of reactor. An ECR region of 875 G was created at the position of ~15 cm above substrates. In the planar ECR plasma system, the resonance magnetic field for ECR was generated by permanent magnets which were arranged in the upper wall. The ECR region of 875 G was created ~6 cm above the substrates. The substrate bias was floating to simulate the chamber cleaning process. O_2 gas was fed through the top of reactor.

The solid material evaporation system consisted of a solid material (PTFE or FEP) target and a continuous wave (cw) CO_2 laser (10.6 μm) used for evaporation of the solid material target. The solid material target was arranged to distance of about 18 cm from the center of chamber. The cw CO_2 laser was very compact (W 70×H 97×L 425 mm; SYNRAD Inc.) and its beam irradiated the surface of PTFE or FEP target in the process chamber through the ZnSe window. The flow rate was successfully controlled by CO_2 laser power. Before starting the evaporation, the process chamber was pumped down to a pressure of 1.33×10^{-3} Pa by a 200 and a 700 *L/s* turbo molecular pump. The evaporation of solid materials was performed at room temperature. The PTFE target of 5 mm in thickness and the FEP target of 10 mm in thickness were used. The melting temperature of PTFE and FEP are 327 and 260 °C, respectively, as shown in Table I. The PTFE and FEP targets were automatically rotated at 333 rpm to be a line speed of about 87 cm/s.

IRLAS is a very powerful diagnostic technique for *in situ* measurement of CF_x ($x=1-3$) radicals in toe plasma without disturbing the plasma.[4–8] White-type multiple reflection cell of 200 cm in length was installed at the process chamber to increase the absorption length of the infrared laser beam used for the radical density measurements. The laser beam passed 12 times for the measurement of CF_2 radical density at 2 cm above the substrate plate through the ECR downstream plasma using White-type multiple reflection cell and 40 times for those of CF, CF_3 radicals densities. Absorption signals were detected by an infrared detector mercury cadmium telluride. The absorption lines used in this study were $R_1(7.5)$ and $R_2(7.5)$ lines for CF radicals,[9] ${}^{Q}R_4(26)$line for CF_2 radicals,[10] ${}^{R}R_{18}(18)$ line for CF_3 radicals.[11] The calculation procedures of radical densities were described in detail in Ref. 4. In these calculation procedures, translational temperatures were calculated from the full width at half maximum of each spectral profile. The translational temperatures were estimated to be ~350 K. It was assumed that the rotational and translational motions of radicals are in thermal

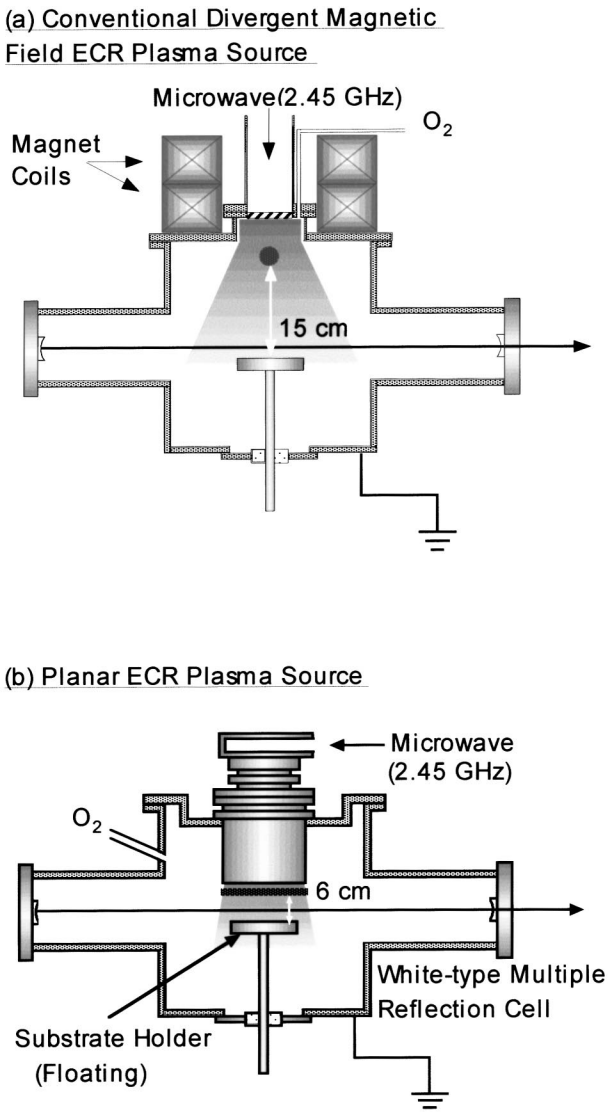

FIG. 1. (a) Conventional divergent magnetic field ECR plasma and (b) the planar ECR plasma process system equipped with a solid material (PTFE or FEP) evaporation system and IRLAS system.

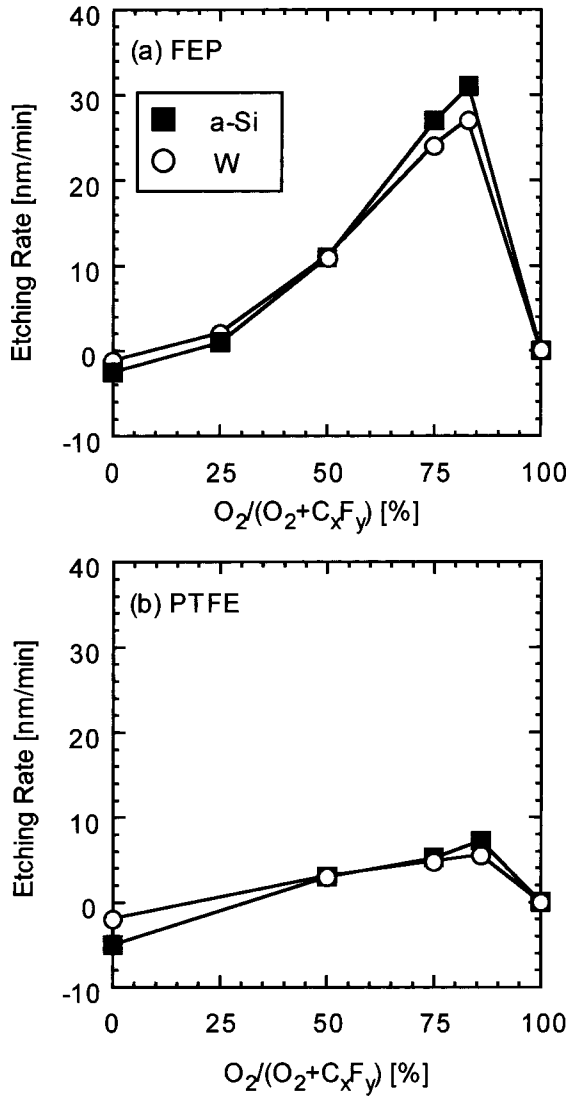

FIG. 2. Etching rates of *a*-Si and W films as functions of O_2 dilution ratio in the conventional divergent magnetic field ECR downstream plasma employing (a) FEP evaporation and (b) PTFE evaporation at a microwave power of 800 W, a pressure of 0.9 Pa, and total flow rate of 36 sccm.

equilibrium, i.e., rotational temperature is equal to translational temperature (~350 K). CF_x (x=1–3) radical densities generated from PTFE and FEP by CO_2 laser evaporation were measured.

In AOES measurements, a compact AOES-plasma monitor (PZ-M2; Opto Research Corp.) was used. Ar gas (concentration ratio: 5%) was added as an actinometer. The measured emission lines of F* and Ar* were $[3s(^2P_2)\text{-}3p(^2P_2)]$ transition at 703.7 nm and $[4s'(1/2)^0 = 4p'(1/2)]$ transition at 750.4 nm, respectively. F atom density was calculated from the emission intensity ratio of F* and Ar*.

The electron densities (n_e) and electron temperatures (T_e) near the substrate were measured with a Langmuir probe. A cylindrical tungsten wire of 0.5 mm in diameter and 10 mm in length extending from a ceramic insulator was used as the Langmuir probe. The probe was positioned at 2

cm above the substrate. The ion bombardment energies were estimated from the difference in floating potential (V_f) and plasma potential (V_p).

III. RESULTS AND DISCUSSION

A. Comparison of solid materials

Etching characteristics between FEP and PTFE used as the evaporation source were investigated using conventional divergent magnetic field ECR O_2 downstream plasma. Figure 2 shows etching rates of *a*-Si and W films as functions of O_2 dilution ratio employing (a) FEP evaporation and (b) PTFE evaporation. In the case of FEP evaporation, *a*-Si and W films were not etched but fluorocarbon films were formed on *a*-Si and W surfaces, at an O_2 dilution ratio of 0%. Etching rates of *a*-Si and W films increased with increasing the O_2 dilution ratio and reached 31 and 27 nm/min at an O_2 dilution ratio of 85%, respectively. At an O_2 dilution ratio of 100%, *a*-Si and W films were not etched. In the case of PTFE evaporation, fluorocarbon films were formed on *a*-Si and W surfaces, at an O_2 dilution ratio of 0%. Etching rates of *a*-Si and W films increased with increasing the O_2 dilution ratio and were 7 and 5 nm/min at an O_2 dilution ratio of 85%, respectively. Etching rates using FEP evaporation were about five times as high as those using PTFE evaporation. It is noteworthy that the FEP has much higher etching rate than PTFE although the FEP has only a little different structure from PTFE with identical atomic composition (F/C=2). These results indicate that etching species in the plasma employing FEP evaporation will be much different from the PTFE one.

In order to obtain the information of reactive species in the conventional divergent magnetic field ECR O_2 downstream plasma employing FEP and PTFE evaporation, CF_x (x=1–3) radical densities and F atom density were measured by AOES and IRLAS, respectively. Figure 3 shows CF_x (x=1–3) radical densities and F atom density as functions of O_2 dilution ratio in the case of (a) FEP evaporation and (b) PTFE evaporation. F atom density was normalized with the value of FEP evaporation at O_2 dilution ratio of 0%. In the case of FEP evaporation, CF, CF_2, and CF_3 radical densities were 2.0×10^{12} cm^{-3}, 1.5×10^{13} cm^{-3}, and 5.0×10^{12} cm^{-3}, respectively at an O_2 dilution ratio of 0%. CF and CF_2 radicals could not be observed at an O_2 dilution ratios above 50% and thus CF and CF_2 radical densities were estimated to be below the detection limit of 1×10^{11} cm^{-3}. CF_3 radical density decreased with increasing the O_2 dilution ratio but more slowly than CF and CF_2 radical densities did. CF_3 radicals could not be observed at an O_2 dilution ratio above 75%. F atom density also decreased slowly with increasing the O_2 dilution ratio. In the case of PTFE evaporation, CF, CF_2, and CF_3 radical densities were 1.6×10^{12} cm^{-3}, 1.7×10^{13} cm^{-3}, and 2.3×10^{12} cm^{-3}, respectively at an O_2 dilution ratio of 0%. CF, CF_2, and CF_3 radical densities rapidly decreased with increasing the O_2 dilution ratio. F atom density also decreased with increasing the O_2 dilution ratio. The absolute values of CF and CF_2 radical densities in PTFE evaporation were almost equal to those in FEP evaporation. It is noteworthy that CF_3 radical density and F atom density in the PTFE evaporation were under half of that in the FEP evaporation. It was considered that F atoms were generated from CF_3 radicals or higher species through the electron impact dissociation and reactions with O radicals. Therefore, higher etching rates were obtained due to higher F atom densities in FEP evaporation.

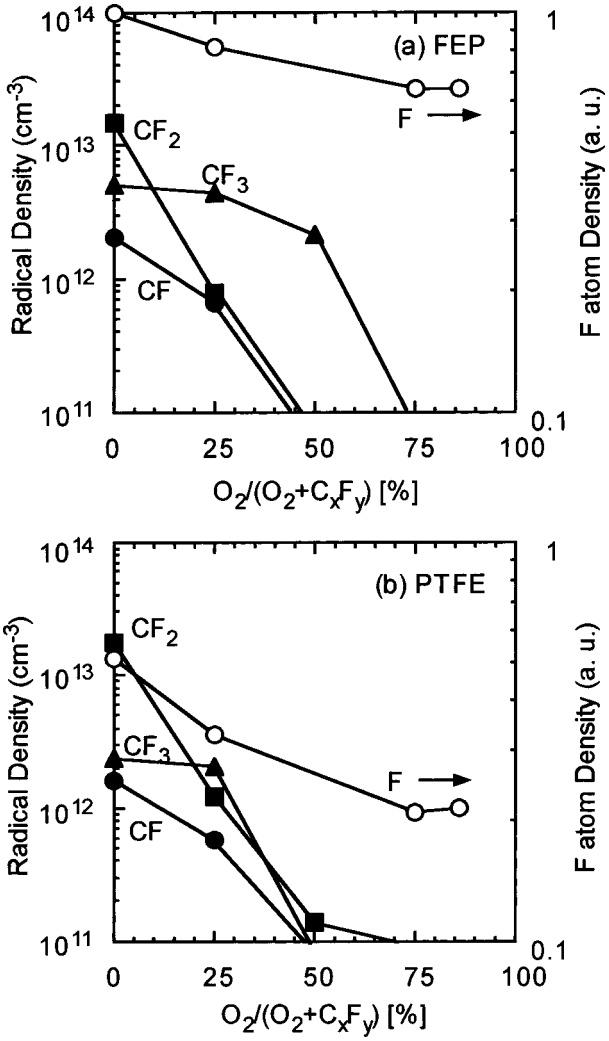

FIG. 3. CF_x (x=1–3) radical densities and F atom density as functions of O_2 dilution ratio in the conventional divergent magnetic field ECR downstream plasma employing (a) FEP evaporation and (b) PTFE evaporation at a microwave power of 800 W, a pressure of 0.9 Pa, and total flow rate of 36 sccm.

In this optimal O_2 dilution ratio of 85%, the dependence of etching rates on pressure was investigated in the conventional divergent magnetic field ECR downstream plasma employing FEP evaporation. Figure 4(a) shows the etching rates of *a*-Si and W films as functions of pressure at an O_2 dilution ratio of 85%. Etching rates of *a*-Si and W films increased with increasing the pressure and reached the maximum at a pressure of 1.6 Pa. At a pressure of 1.6 Pa, etching rates of *a*-Si and W films were about 47 and 55 nm/min, respectively. Etching rates of *a*-Si and W films decreased at pressures above 2.7 Pa. In order to explain these phenomena, F atom

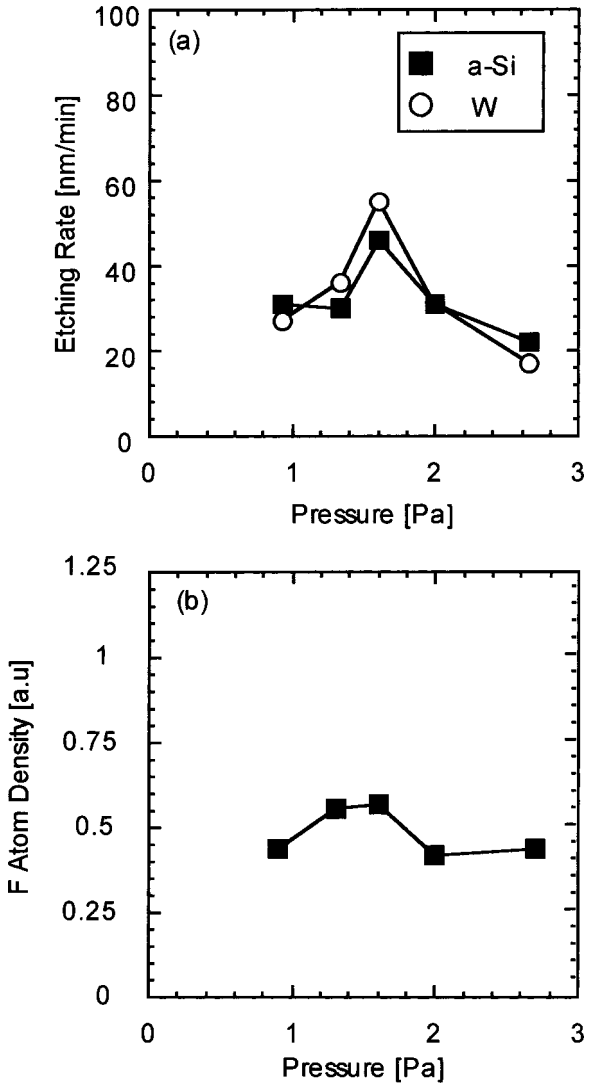

FIG. 4. (a) Etching rates of *a*-Si and W films as functions of pressure in the conventional divergent magnetic field ECR downstream plasma employing FEP evaporation at an O_2 dilution ratio of 85%, a microwave power of 800 W, and total flow rate of 36 sccm. (b) F atom density as a function of pressure.

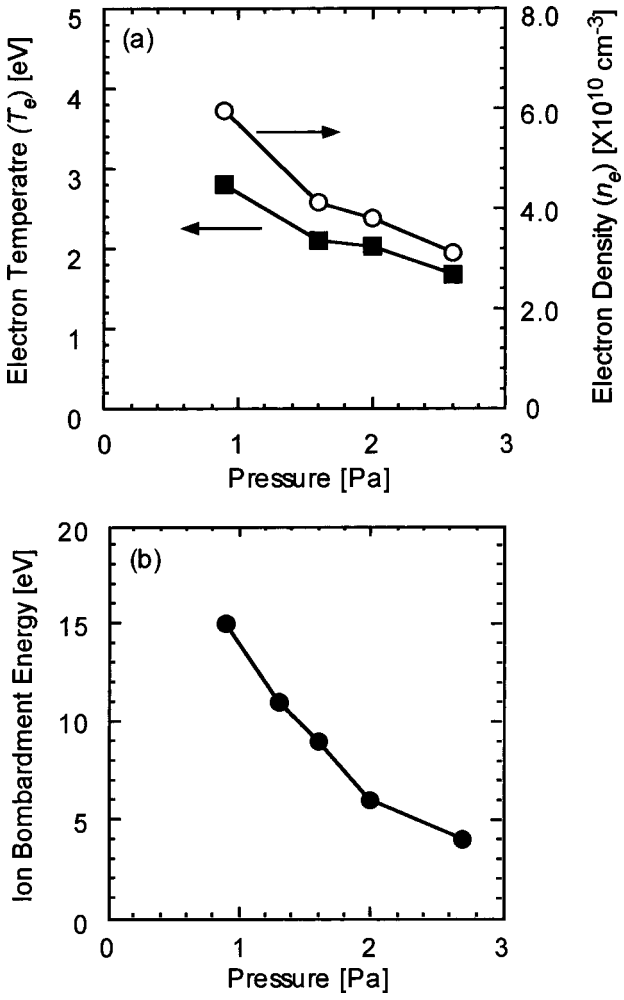

FIG. 5. (a) T_e and n_e as functions of pressure in the conventional divergent magnetic field ECR downstream plasma employing FEP evaporation at an O_2 dilution ratio of 85%, a microwave power of 800 W, and total flow rate of 36 sccm. (b) The ion bombardment energy estimated from the difference in V_f and V_p as functions of pressure.

and CF_x (x=1–3) radical densities were measured by AOES and IRLAS, respectively. CF_x (x=1–3) radical densities could not be observed at any pressures and thus those were lower than the detection limit of 1×10^{11} cm^{-3}. It was considered that these decreases were caused by decreasing the partial pressure of fluorocarbon species and/or reacting with oxygen atoms in the plasma. Figure 4(b) shows the F atom density as a function of pressure. F atom density increased with increasing the pressure and reached the maximum at a pressure of 1.6 Pa. The behavior of F atom density below 1.6 Pa is roughly similar to that of etching rate as shown in Fig. 4(a). The small discrepancy seen between behaviors of F atom density and etching rate will be due to the measurement errors of actinometry and tally step method. However, the decrease of etching rates above 1.6 Pa is not explained by only the behavior of F atom density.

In order to clarify the behavior of etching rates as shown in Fig. 4(a), T_e and n_e in the conventional divergent magnetic field ECR downstream plasma employing FEP evaporation were measured by using a Langmuir probe. Figure 5(a) shows T_e and n_e in the conventional divergent magnetic field ECR downstream plasma employing FEP evaporation as functions of pressure. The T_e decreased from 2.8 to 1.5 eV and the n_e decreased from 6.0×10^{10} cm^{-3} to 1.4×10^{10} cm^{-3} with increasing the pressure. From these results, it is considered that F atom density decreased at pressures above 1.6 Pa due to decreases of T_e and n_e. Figure 5(b) shows the ion bombardment energy estimated from the difference in V_f and V_p as a function of pressure. Ion bombardment energy was estimated to be 15 eV at a pressure of 0.9 Pa. Ion bombardment energy decreased with increasing the pressure and was 4 eV at a pressure of 3.9 Pa. From these results, the following etching model of *a*-Si and W films is considered. F atoms react with surfaces of *a*-Si and W films, and the subsequent ion bombardment forms volatile gas-phase products such as SiF_x, WF_6, and WOF_x. Therefore it is considered the rate limiting step below 1.6 Pa will be due

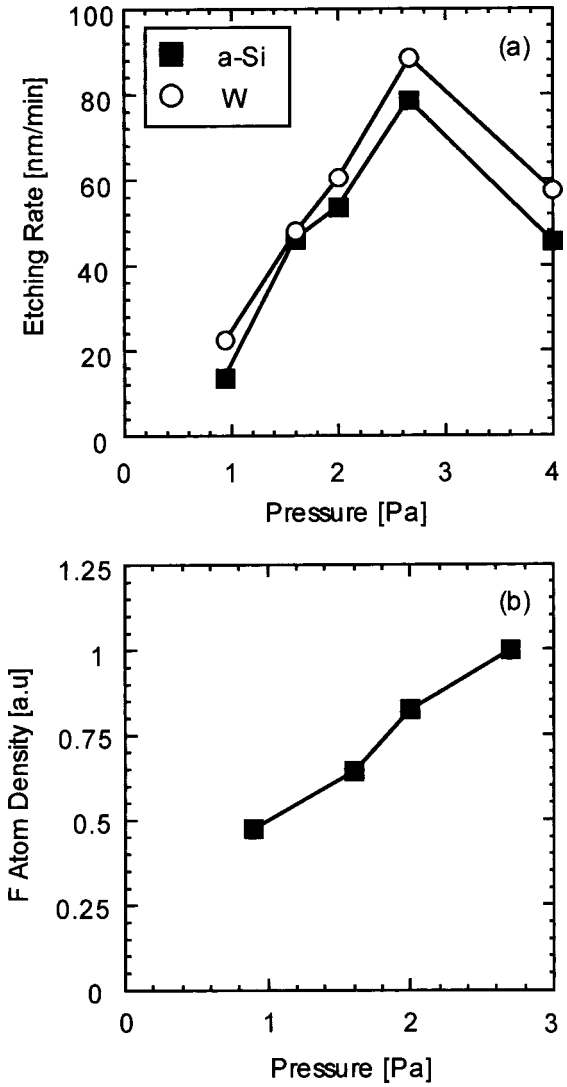

FIG. 6. (a) Etching rates of *a*-Si and W films in planar ECR plasma employing FEP evaporation as functions of pressure at an O_2 dilution ratio of 85%, a microwave power of 400 W, and total flow rate of 36 sccm. (b) The F atom density in planar ECR plasma source as a function of pressure.

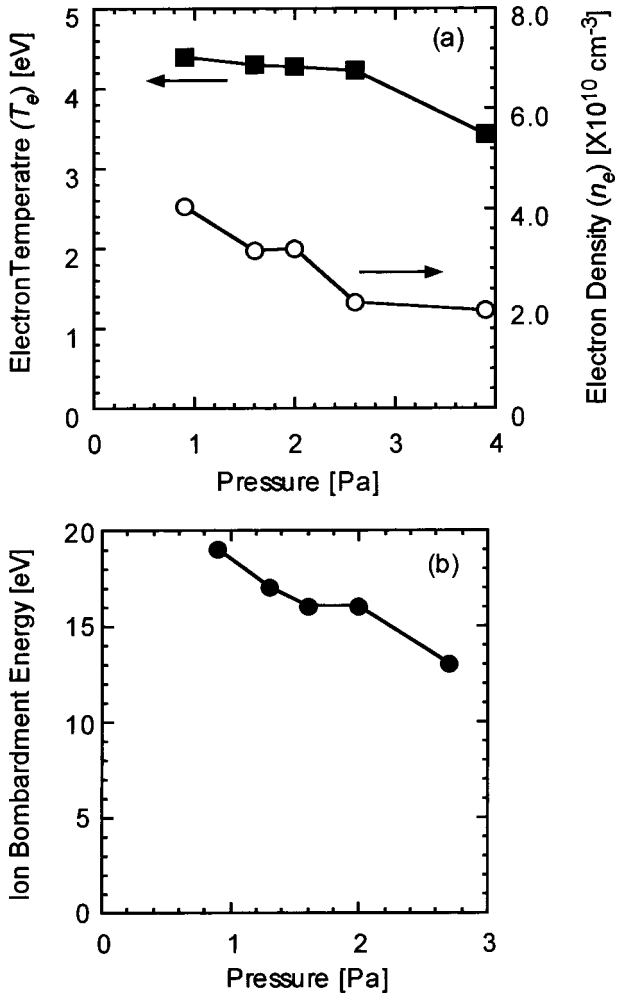

FIG. 7. (a) T_e and n_e in planar ECR plasma employing FEP evaporation as functions of pressure at an O_2 dilution ratio of 85%, a microwave power of 400 W, and total flow rate of 36 sccm. (b) The ion bombardment energy estimated from the difference in V_f and V_p as functions of pressure.

to F atom density while that above 1.6 Pa will be due to ion flux and energetic ion bombardment in addition to F atom density.

B. Dependence on plasma source

Using the FEP evaporation, etching characteristics employing the planar ECR plasma source were compared with those employing the conventional ECR downstream plasma source. Plasma densities of the two plasma sources were controlled to be almost equal by changing microwave power. Figure 6(a) shows the etching rates of *a*-Si and W films as functions of pressure in the planar ECR plasma employing FEP evaporation. Etching rates of *a*-Si and W films increased with increasing the pressure and reached the maximum at a pressure of 2.7 Pa. At a pressure of 2.7 Pa, etching rates of *a*-Si and W films were about 78 and 87 nm/min, respectively. Etching rates of *a*-Si and W films decreased with increasing the pressure up to 3.9 Pa. The behavior of etching rates was different between using a planar ECR plasma source and using a conventional one. Etching rates of *a*-Si and W films using a planar ECR plasma source are higher than those using a conventional one. Figure 6(b) shows F atom density using a planar ECR plasma source as a function of pressure. F atom density increased with increasing the pressure. Furthermore, F atom densities using a planar ECR plasma source were high compared with those using a conventional ECR plasma source should in Fig. 4(b). CF_x (x=1–3) radical densities could not be observed at any pressures and thus those were lower than the detection limit of 1×10^{11} cm^{-3}. Therefore, higher etching rates of *a*-Si and W films using a planar ECR plasma source will be mainly due to higher densities of F atom as described before.

In order to discuss the difference of F atom densities between the two type plasma sources, T_e and n_e were measured using single probe method. Figure 7(a) shows the T_e and n_e in planar ECR plasma employing FEP evaporation as functions of pressure. The T_e decreased slowly from 4.4 to 3.4 eV and the n_e also decreased slowly from 4.0×10^{10} cm^{-3} to

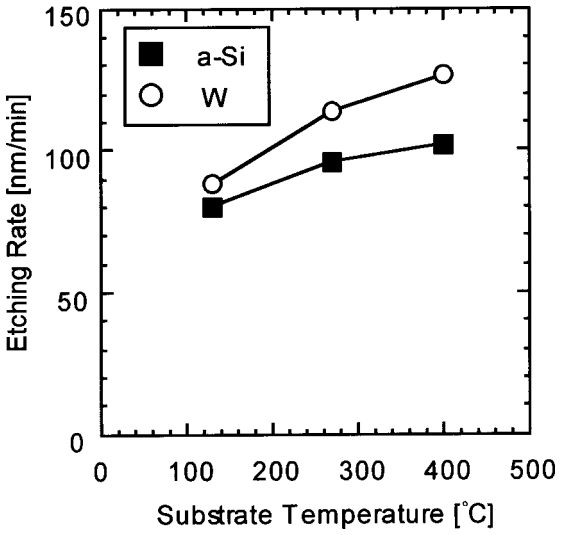

FIG. 8. Etching rates of *a*-Si and W films as functions of substrate temperature in planar ECR plasma employing FEP evaporation at an O_2 dilution ratio of 85%, a microwave power of 400 W, and total flow rate of 36 sccm.

1.9×10^{10} cm^{-3} with increasing the pressure. From these results, it was found that T_e in the planar ECR plasma source was high compared with that in the conventional ECR plasma source, while the n_e was almost equal. Therefore, F atoms were efficiently generated by using high T_e plasma source. Figure 7(b) shows ion bombardment energy in planar ECR plasma employing FEP evaporation as a function of pressure. Ion bombardment energy decreases slowly from 19 to 13 eV with increasing the pressure. Therefore, etching rates of *a*-Si and W films below 2.7 Pa are determined by F atom density. However, etching rates above 2.7 Pa are determined by not only F atom density but also ion flux and energetic ion bombardment since F atom density increased with increasing the pressure.

C. Effect of substrate heating

The substrate temperature during etching is a very important factor in controlling the etching characteristics. In order to investigate the dependence of etching rates of *a*-Si and W films on the substrate temperature, the substrate temperature was changed from 120 to 400 °C in planar ECR plasma employing FEP evaporation. Figure 8 shows the etching rates of *a*-Si and W films as a function of substrate temperature in planar ECR plasma employing FEP evaporation. Etching rates of *a*-Si and W films increased linearly with increasing the substrate temperature. The etching rates of *a*-Si and W films at a substrate temperature of 400 °C were 102 and 127 nm/min, respectively. It is considered that the surface reaction of reactive species was enhanced, and vapor pressures of by-products increase due to the increase of substrate temperature. Therefore, it is important to control the reactor wall temperature for increasing the etching rates of *a*-Si and W films in the chamber cleaning process.

IV. CONCLUSIONS

Environmentally benign etching process of *a*-Si and W films by using O_2 plasma with a solid material evaporation system has been developed for replacing the conventional process using green house gases, such as SF_6 gas and PFC gases causing global warming. The solid material evaporation system was designed to generate fluorocarbon species from solid materials by a CO_2 laser evaporation. The ECR O_2 plasma equipped with the solid material evaporation system has been applied to *a*-Si and W etching for chamber cleaning process after CVD. FEP and PTFE were selected as the solid material for the evaporation and the etching characteristics using FEP were compared with those using PTFE in the conventional divergent magnetic field ECR downstream plasma. As a result, etching rates using FEP evaporation were about five times as high as those using PTFE evaporation and etching rates of *a*-Si and W films were 31 and 27 nm/min, respectively. It is noteworthy that the FEP has much higher etching rate than PTFE although the FEP has only a little different structure from PTFE with identical atomic composition (F/C=2). Therefore, this process using solid materials is very interesting from a viewpoint of new gas chemistry.

Furthermore, effects of plasma characteristics in the FEP evaporation were investigated using two types of plasma sources of the divergent magnetic field ECR downstream plasma [n_e;$\sim10^{10}$ cm^{-3}, Te; 1.5–2.8 eV] and a planar ECR plasma [n_e;$\sim10^{10}$ cm^{-3}, T_e; 3.4–4.4 eV] using O_2 gas with FEP evaporation. High etching rates of *a*-Si and W films of above 100 nm/min were successfully obtained at a substrate temperature of 400 °C in the planar ECR plasma of higher electron temperature. From these results, it was found that higher etching rates were obtained with high T_e plasma source, which was due to high densities of F atoms, and with high substrate temperature. These results indicated that this technique has a great potential to be applicable to a chamber cleaning process with new gas chemistry for replacing the conventional process with green house gases.

ACKNOWLEDGMENTS

This work is (partly) supported by the ''Research for the Future'' Program (No. JSPS-RFTF96R13101) of the Japan Society for the Promotion of Science. This work is also partially supported by NEDO. The authors would also like to thank T. Ohkura in Opto Research Corporation for the use of AOES-plasma monitor. The authors also would like to sincerely thank Dr. Shoji Den of Katagiri Engineering Co., Ltd. for helpful advice and discussions in the planar ECR plasma system.

[1]K. Fujita, M. Ito, M. Hori, and T. Goto, J. Vac. Sci. Technol. B **17**, 957 (1999).
[2]K. Fujita, M. Ito, M. Hori, and T. Goto, J. Vac. Sci. Technol. A **17**, 3260 (1999).
[3]K. Fujita, S. Kobayashi, M. Ito, M. Hori, and T. Goto, Mater. Sci. Semicond. Process. **2**, 219 (1999).
[4]M. Magane, N. Itabashi, N. Nishiwaki, T. Goto, C. Yamada, and E. Hirota, J. Appl. Phys. **29**, L829 (1990).

[5]K. Maruyama, K. Ohkouchi, Y. Ohtsu, and T. Goto, Jpn. J. Appl. Phys., Part 1 **33**, 4298 (1994).
[6]K. Takahashi, M. Hori, and T. Goto, Jpn. J. Appl. Phys., Part 1 **33**, 4745 (1994).
[7]K. Miyata, K. Takahashi, S. Kishimoto, M. Hori, and T. Goto, Jpn. J. Appl. Phys., Part 2 **34**, L444 (1995).
[8]K. Miyata, M. Hori, and T. Goto, J. Vac. Sci. Technol. A **14**, 2343 (1996).
[9]K. Kawaguchi, C. Yamada, Y. Hamada, and E. Hirota, J. Mol. Spectrosc. **102**, 193 (1983).
[10]P. B. Davies, W. Lewis-Bevan, and D. K. Russell, J. Chem. Phys. **75**, 5602 (1981).
[11]C. Yamada and E. Hirota, J. Chem. Phys. **78**, 1703 (1983).